Proceedings World Geothermal Congress 2023
Beijing, China, October 9-11, 2023

Main Controlling Factors of Formation Temperature Difference in the Shuntuoguole Area, Tarim Basin, NW China

Keyan Liao. Author, Nansheng Qiu

College of Geosciences, China University of Petroleum, Beijing 102249, China.

liaoky2023@163.com

Keywords: Tarim Basin, Shuntuoguole, Heat flow, Crustal structure

ABSTRACT

The Tarim Basin has a relatively low surface heat flow (~42.5mW m^{-2}), but the change of formation temperature is still obvious. Shuntuoguole area is located in the center of the basin. Based on the steady temperature measurement data of 34 wells, we obtained that the average temperature gradient of 0–5 km in the south and north of the Shuntuoguole area is 22.5 ℃ km^{-1} and 18.6 ℃ km^{-1} respectively. In combination with temperature measurement, thermophysical properties, logging and geophysical data, this study calculates the effective thermal conductivity and heat generation rate of the sedimentary layer of representative wells, constructs the crustal structure of the two areas, and compares the crustal heat flow. We have found that the structure of the basement crust is the main controlling factor for the formation temperature. The influence of thermophysical properties of sedimentary layer and basement morphology is not significant, and the effects of rapid sedimentation and hydrothermal activity has disappeared. The low mantle heat flow (12.5 mW m^{-2}) is related to the thicker thermal lithosphere in the stable cratonic basin.

1. INTRODUCTION

The research of formation temperature in sedimentary basin is helpful to understand basin formation and tectonic evolution. On the one hand, the formation temperature is controlled by the dual geodynamic processes of deep thermodynamic process and shallow basin tectonic evolution (Cloetingh et al. 2010; Melouah et al. 2021; Qiu et al. 2022). On the other hand, it is also affected by factors such as rock thermophysical properties and fluid activities (Hasterok and Chapman 2011; Sippel et al. 2015; Maytrenko et al. 2015). The deep exploration wells in oil and gas exploration can not only provide the information of deep geological structure, stratum and reservoir properties, but also provide the information of deep temperature. Various geophysical data also provide a basis for interpreting the lithospheric structure. At present, the study of formation temperature is limited to the description of characteristics, and the study of control factors is less. It is very important to know the controlling factors of the formation temperature for grasping the temperature distribution law and predicting the deep layer temperature.

Shuntuoguole area has superior hydrocarbon accumulation conditions, but there are great differences in hydrocarbon enrichment types. Taking Ordovician oil and gas reservoirs as an example, Shunnan area (the southern Shuntuoguole Low Uplift) is dominated by dry gas reservoirs and condensate gas reservoirs, while Shunbei area (the northern Shuntuoguole Low Uplift) is dominated by light oil reservoirs (Qi 2016; Ma et al. 2022). The temperature measurement data shows that the average temperature of the strata in the Shunnan area is about 30 ℃ higher than that in the Shunbei area at a depth of 7,000m (Liu et al. 2020). Therefore, temperature difference may be the main reason for the difference of oil and gas reservoir types (Chen et al. 2020). Wan et al. (2017) believed that the uplift of the basement formed a high temperature gradient in the Shunnan area. Liu et al. (2020) also believes that the basement tectonic setting is the main controlling factor of the current formation temperature, and analyzes the disturbance of the Cenozoic hydrothermal activity in the Shunnan area to the deep strata. However, the influence of basement morphology needs quantitative study, and the hydrothermal activity along the fault is also difficult to cause regional temperature anomaly. In a word, the controlling factors of formation temperature in Shuntuoguole area need further study.

This study compares the geological conditions of Shunnan and Shunbei areas regions from shallow to deep, and analyzes the controlling factors of formation temperature in many aspects. Based on the characteristics of temperature gradient, we selected representative wells in the two regions, and compared the thermal conductivity and heat generation rate of the sedimentary layers in sections. On the basis of analyzing the crustal structure, we calculated the heat flow of the crust. In addition, we also discussed the effects of rapid deposition, hydrothermal activity and basement morphology, and the causes of low mantle heat flow.

2. GEOLOGICAL BACKGROUND

The tectonic position of Shuntuoguole area refers to the low uplift and surrounding area of Shuntuoguole. Shuntuoguole low uplift is located in the central of Tarim Basin, between Tazhong uplift and Tabei uplift in the north and south, and between Awati depression and Manjiar depression in the east and west (Fig. 1). Shuntuoguole low uplift mainly includes four secondary structural units: Shunbei area, Shuntuo area, Shundong area and Shunnan area (Ma et al. 2012; Jiao 2017).

Shuntuoguole low uplift was initially formed in the Middle-Late Ordovician, and formed a monoclinal structure with high southeast and low northwest through Caledonian collision orogeny in the Middle Silurian (Li et al. 2009). After the Late Devonian, the structure in this area has been in a stable state without being damaged by tectonic movement (He et al. 2008; An et al. 2009; Deng et al. 2019). The structural deformation of the Shuntuoguole low uplift is weak (Fig. 1b), and a series of NE and NEE strike slip faults are developed (Jiao 2017; Deng et al. 2018; Deng et al. 2019). The main active period of these faults is from late Caledonian to early Hercynian. Later, weak activities occurred under compression and tensile stress (Huang 2014, Jiao 2017). The NE strike slip fault has the largest scale of development, and some of it breaks through from the basement to the bottom of the middle and lower Devonian, controlled by the pre-existing basement weak zone, the middle and lower Cambrian gypsum salt rock detachment zone, and basin mountain coupling in different periods (Huang 2014; Zhang et al. 2018).

Shuntuoguole low uplift experienced marine sedimentary environment from Cambrian to early Permian and continental sedimentary environment from late Permian to Quaternary (Jia and Wei 2002). At present, the average thickness of the sedimentary layer in the low uplift of Shuntuoguole is more than 10 km (Fig. 1c). Except for the lack of Jurassic system in the region, Silurian and Devonian systems are missing to varying degrees due to the evolution of Guchengxu uplift (Huang 2014).

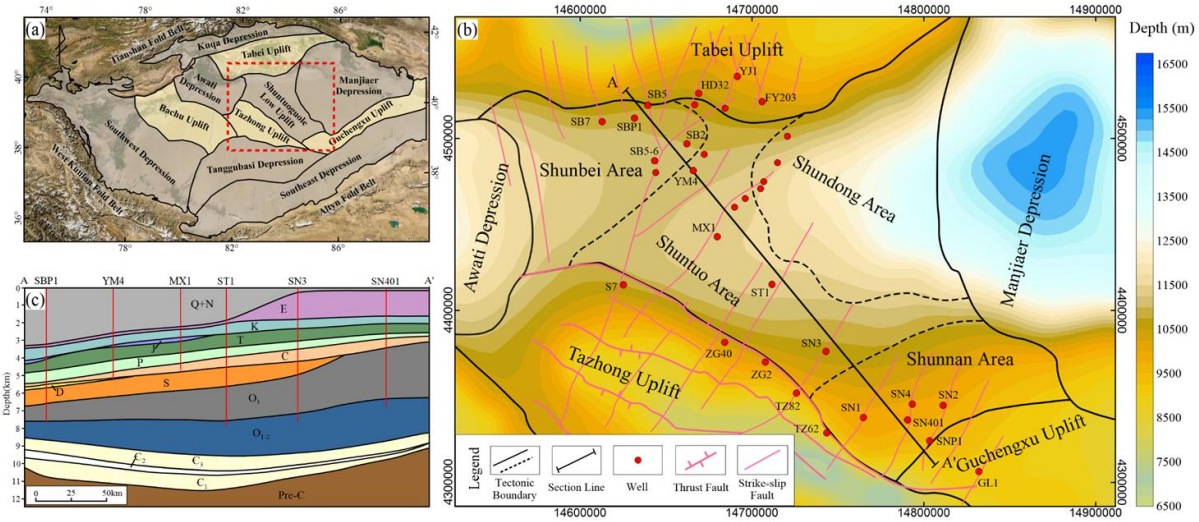

Figure 1: (a)Tectonic Division of Tarim Basin and Location Map of Study Area; (b) Structural division and basement burial depth map of Shuntuoguole area; (c) Stratigraphic profile (see (b) for the location of the profile line).

3. DATA AND METHODS

The continuous steady temperature measurement data of 34 wells in the Shuntuoguole area were collected to calculate the temperature gradient (Fig. 2). The continuous steady temperature is the temperature data obtained by continuous measurement of the whole borehole or specific well section for several months or even years after the well is shut down, so it can best reflect the real underground temperature (Liu et al. 2017). The evaluation of thermal conductivity is based on the previous test results of rock samples in Tarim Basin (Wang et al. 1995; Qiu 2002; Feng et al. 2009; Li et al. 2019; Liu et al. 2020).

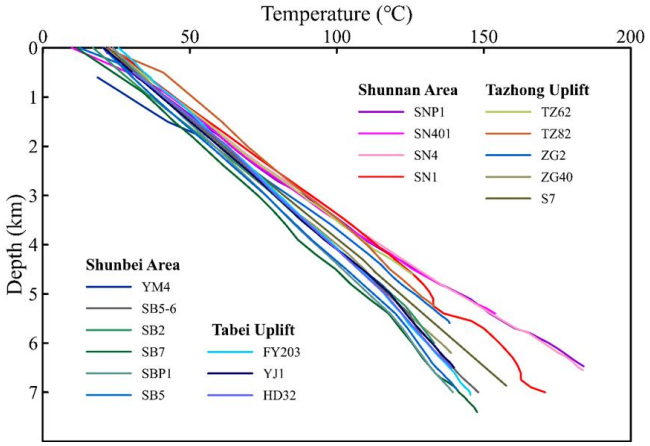

Figure 1: (a)Tectonic Division of Tarim Basin and Location Map of Study Area; (b) Structural division and basement burial depth map of Shuntuoguole area; (c) Stratigraphic profile (see (b) for the location of the profile line).

The heat generation rate is obtained by using the empirical formula proposed by Bucker and Rybach (1996):

$$A = 0.0158(GR - 0.8) \quad (1)$$

Where, A is the heat generation rate, $\mu W\ m^{-3}$; GR is the natural gamma logging value, API.

In this study, linear decline theory is used to characterize the relationship between heat flow and heat generation rate (Roy et al. 1968; Beardsmore and Cull 2001; Jaupart and Mareschl 2010):

$$Q = G\lambda + \frac{AZ}{2} \quad (2)$$

Where: Q is the top heat flow, mW m^{-2}; G is temperature gradient, ℃ km^{-1}; λ is the average thermal conductivity, W m^{-1} K^{-1}; Z is the thickness, km. In order to reduce the error, the stratum section far from the surface and with simple lithology is selected to calculate the heat flow. In addition, when the top heat flow is known, the calculation formula of bottom heat flow Q_Z (mW m^{-2}) is:

$$Q_Z = Q - AZ \tag{3}$$

When the top heat flow, temperature gradient and heat generation rate are known, the effective thermal conductivity of the formation can be calculated according to Formula 2.

Crustal structure refers to previous researches on basin geophysics and petrology. On this basis, we have established the crustal stratification model and heat flow structure.

4. RESULTS

4.1 Temperature Gradient

Based on the temperature measurement data, we calculated the temperature gradient distribution map of the 0–5 km depth section (Fig. 3). There is a significant difference in temperature gradient in the area of Shuntuoguole, and the temperature gradient gradually increases from Shunnan area to Shunbei area. The temperature gradient in the Shunnan area is 21.5–24.5 ℃ km^{-1}, with an average of ~22.5 ℃ km^{-1}. The temperature gradient in the Shunbei area is 17.5–20.0 ℃ km^{-1}, with an average of ~18.6 ℃ km^{-1}. There are also changes in the interior of Shunnan and Shunbei areas. In the Shunnan area, Wells SNP1 and SN401 are the high value centers, and the temperature gradient gradually decreases around. Wells SBP1 and SB2 in the Shunbei area have relatively low and high temperature gradients respectively. In order to facilitate comparative analysis, Wells SN1 and SB7 are selected as representative wells in the Shunnan and Shunbei areas for further research. The temperature gradient of these two wells is close to the average temperature gradient of their respective blocks, which is representative.

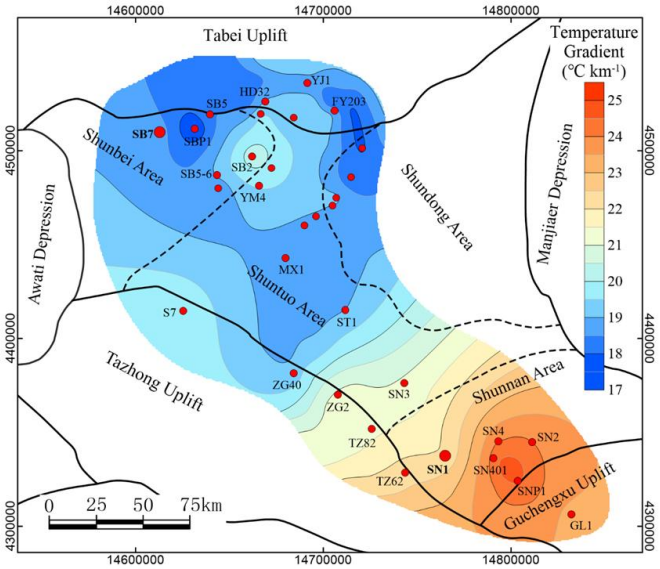

Figure 3: Temperature Data from Continuous Steady State of Shuntuoguole low uplift and Its Surroundings.

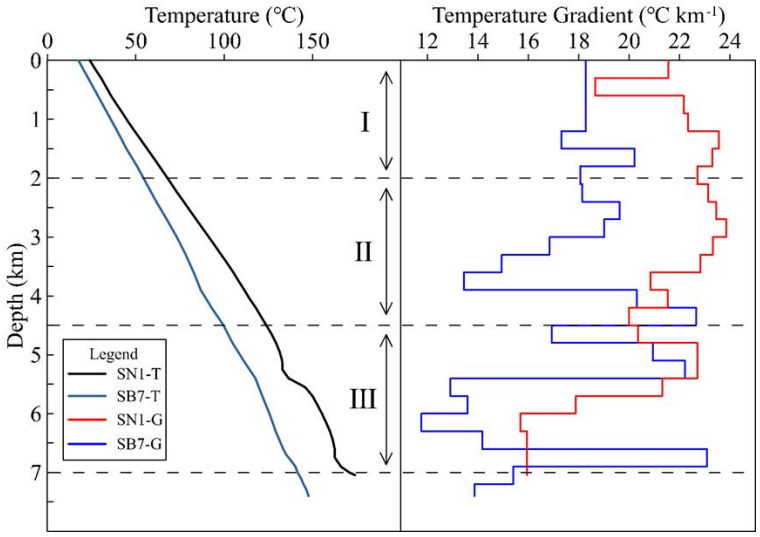

Figure 4: The relationship between temperature and depth, temperature gradient and depth of wells SN1 and SB7.

4.2 Thermophysical Properties of Sedimentary Layer

The temperature curves of representative wells SN1 and SB7 show significant differences in shallow temperature (Fig. 4). The curves are segmented according to the depth, which are section I (0–2.0 km), II (2.0–4.5 km), and III (4.5–7.0 km) respectively. The formation of section II is far from the surface, there is no special stratum. The formation lithology is mainly sandstone and mudstone. Figure 5 summarizes the lithology, thermal conductivity and heat generation rate of the representative well section II.

The thermal conductivity, heat generation rate and heat flow of each depth section of the sedimentary layer calculated according to the above method are shown in Table 1. In terms of thermal conductivity, the difference between the thermal conductivity of the representative well section I and II is less than 0.20 W m^{-1} K^{-1}, which is not significant. The thermal conductivity of section III of SN1 well is obviously higher than that of SB7 well. Logging records of section III show that well SN1 is mainly composed of Ordovician mudstone and limestone, while well SB7 is composed of sandstone and mudstone, and Permian dacite (1.78 W m^{-1} K^{-1}) and tuff (1.47 W m^{-1} K^{-1}) about 680m thick. In terms of heat generation rate, the heat generation rate of SB7 well section I and II is higher than that of SN1 well, which may be related to the huge thickness of Cenozoic sediments in the Shunbei area; The third section of both wells has high heat generation rate, which is related to the Upper Ordovician mudstone (1.73 μW m^{-3}) in the Shunnan area and the Permian igneous rock (2.00 μW m^{-3}) in the Shunbei area. The sedimentary strata not reached by the well are determined by the lithological composition and thermophysical properties according to the research results of the basin area (Fan et al. 2021), and the depth of the sedimentary bottom is obtained from seismic data (Yang et al. 2022). Sedimentary strata with a depth of more than 7km in the study area are mainly composed of Ordovician limestone, Cambrian dolomite and thin layer gypsum salt rock, with high thermal conductivity and low heat generation rate.

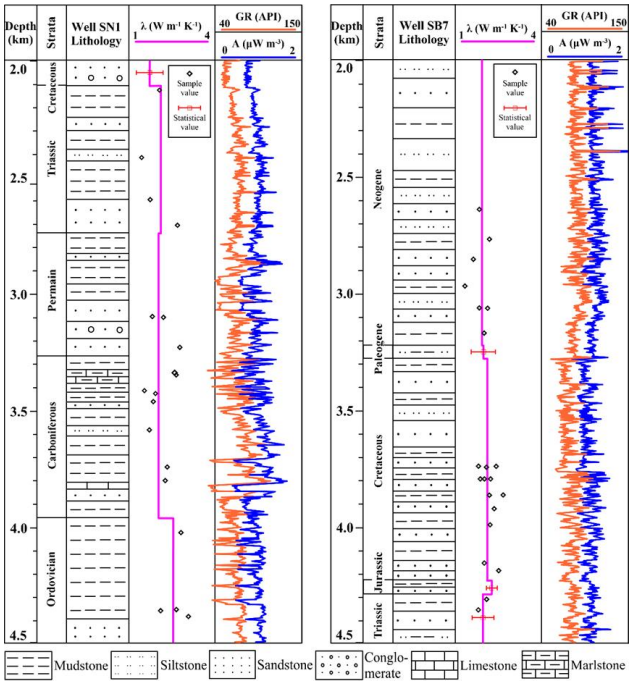

Figure 5: Summary of lithology, thermal conductivity and heat generation rate of formation at 2–4.5 km depth of wells SN1 and SB7.

Table 2: Lithology and heat generation rate of each crustal layer of the basement.

Well	Depth Section (km)	Symbol	Temperature gradient (°C km^{-1})	Thermal conductivity (W m^{-1} K^{-1})	Heat generation rate (μW m^{-3})	Top heat flow (mW m^{-2})
SN1	0.0-2.0	I	22.0	2.20	0.75	49.1
	2.0-4.5	II	22.3	2.08	0.95	47.6
	4.5-7.0	III	18.8	2.31	1.45	45.3
	7.0-10.0			3.34	0.73	41.6
	Basement					39.4
SB7	0.0-2.0	I	18.4	2.04	1.01	38.7
	2.0-4.5	II	18.1	1.94	1.22	36.7
	4.5-7.0	III	16.8	1.90	1.43	33.6
	7.0-10.9			3.28	0.75	30.1
	Basement					27.1

According to the calculation results of thermophysical properties, the average thermal conductivity of the sedimentary layers of the representative wells in the Shunnan and Shunbei areas are 2.44 W m^{-1} K^{-1} and 2.30 W m^{-1} K^{-1} respectively. The average heat generation rate is 0.97 μW m^{-3} and 1.06 μW m^{-3}。 The heat flow generated by the sedimentary layer is 9.7 mW m^{-2} and 11.6 mW m^{-2} respectively. There is no significant difference in thermophysical properties of sedimentary layers. Compared with the surface heat flow, the heat flow at the bottom of the Shunnan and Shunbei areas sedimentary layers shows greater difference. Therefore, the difference of thermophysical properties of sedimentary rocks is not the main controlling factor for the difference of formation temperature in the study area.

4.3 Crustal Heat Flow

The surface heat flow is the sum of the crust heat flow and the mantle heat flow. In a stable continental region, the heat flow from the mantle varies in a large wavelength range. Jaupart and Mareschal (2015a) pointed out that the mantle heat flow of Precambrian craton is basically unchanged within a certain distance (400–500 km). Therefore, when interpreting the change of surface heat flow in the study area, only the difference within the crust needs to be considered.

4.3.1 Crustal Structure

The crust of a sedimentary basin consists of sedimentary layer and crystalline basement, which usually refers to the metamorphic rock stratum between the Cambrian bottom and Moho. The Tarim Basin has extremely thick Phanerozoic strata, more than 15 km in some parts, which hinders direct observation of the structure and evolution history of the basement. Therefore, the structural interpretation of the basement is either based on geophysical data (Xu et al. 2005; He et al. 2011; Gao et al. 2015; Kuang et al. 2022), or based on surface geological inference and sample analysis at the basin margin (Zheng et al. 2010; Zhou et al. 2011; Yang et al. 2018). In addition, a few deep wells drilled to the basement in the basin also provide important support for basement research (Li et al. 2003; Guo et al. 2005; Yang et al. 2018). The aeromagnetic ΔTa anomaly shows that a significant east–west high value anomaly zone crosses Shuntuo area (Xu 1997; He et al. 2011), separating Shunnan and Shunbei areas (Figure 6). The magnetic intensity of this anomaly zone is 100–350 nT, the length can reach to 1500km, and the width is 30–100 km (Xu 1997). Through the upward prolongement process from 20 km to 75 km, the anomaly zone still retains the high magnetic anomaly, indicating a large range of magnetic sources with strong magnetism (Li et al. 2014). The central high aeromagnetic anomaly zone was interpreted by some scholars as the splicing zone of the northern and southern Tarim terranes (Wu et al. 2012; Yang et al. 2018). The geological characteristics and volcanic activity of the basement indicate that these two terranes have experienced independent evolution in Precambrian (Yang et al. 2014; Zhu et al. 2021). In the process of evolution, the southern terrane has undergone multiple metamorphism and igneous activities, both mafic and granitoid igneous rock intrusions have occurred (Yang et al. 2018; He et al. 2019), while the northern terrane has weak metamorphism and volcanic activities, and only mafic igneous rock intrusions have been found (Zhu et al. 2021).

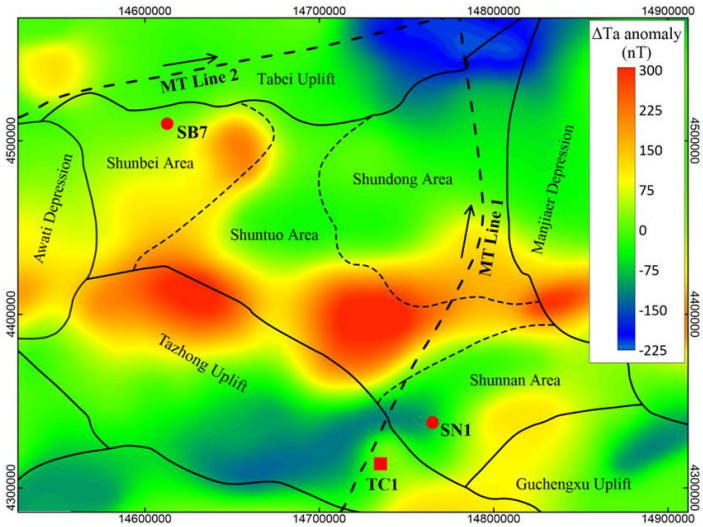

Figure 6: Distribution map of aeromagnetic ΔTa anomaly in Shuntuoguole area (modified from Xu 1997).

Well TC1, located near Shunnan area (Fig. 6), drilled through the Precambrian basement, and the analysis results of basement samples are intrusions of granite and granodiorite (Yang et al. 2018; Li et al. 2003). The granite type is I–type granite mixed with crust and a small amount of mantle (Li et al. 2005). The formation process of intrusion is related to crustal collision and subduction events (Guo et al. 2005; Yang et al. 2018; Shi et al. 2018; He et al. 2019). Geochemical characteristics indicate that the Ordovician quartz vein fluid in well SN4 has basement magmatic rock materials (Chen et al. 2016).

All these evidences indicate that granitoid intrusions may exist in the basement of Shunnan area. In the process of assembling the Tarim terranes, the oceanic crust basement in the middle subducted toward the lower part of the terranes (Shi et al. 2018). Metabasalts collected in Aksu area at the northwest edge of the basin show the geochemical characteristics of oceanic crust basalt (Zheng et al. 2010; Zhu et al. 2021). The northern depression is on the residual oceanic crust between Bachu-Southeast united ancient land and the northern ancient land (Yang et al. 2021), and its crust has relatively high seismic wave velocity and magnetic susceptibility (Wang et al. 2019; Kuang et al. 2022). According to the principle of equilibrium adjustment (Hsü 1958), the depression with the residual oceanic crust as the bottom will deposit and fill the thickest stratum (Xu 1993).

Up to now, 9 magnetotelluric (MT) profiles have been deployed in the Tarim Basin (Yang et al. 2021; Yang et al. 2022). According to the research results of stratigraphic chronology and geochemistry and other geophysical data, the MT line passing through the study area has been interpreted geologically (Fig. 7). Moho depth adopts the results explained by Teng et al. (2013). As shown in Fig. 7a, the joint of Tarim terrain is inclined to the south, and the northern terrain tends to subduct to the lower part of the southern terrain. There are obviously different types of basement crust in the Shunnan and Shunbei areas. The basement in the Shunnan area has complete Archean-Proterozoic strata. Large scale granitoid intrusions exist in the crust and are characterized by longitudinal puncture. The basement in the Shunbei area shows that the Mesoproterozoic directly covers the ocean crust, lacking Archean-Paleoproterozoic layers, and the volcanic activity is weak (Fig. 7b).

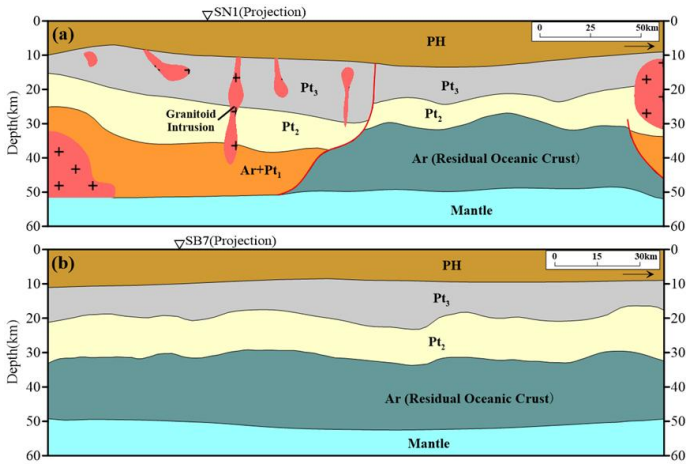

Figure 7: Geological interpretation map of magnetotelluric MT (a) line 1 and (b) line 2 (the location of the line is shown in Figure 6; modified from Yang et al. 2021).

4.3.2 Heat Flow

The crustal structure controls the distribution of radioactive heat generating elements, thus affecting the heat flow structure of the basement. On this basis, the crustal stratification model of representative wells in the Shunnan and Shunbei areas is established (Fig. 8). The lithology and heat generation rate of each layer is determined based on previous studies (Table 2; Mareschal and Jaupart 2013; Yang et al. 2014; Liu et al. 2017).

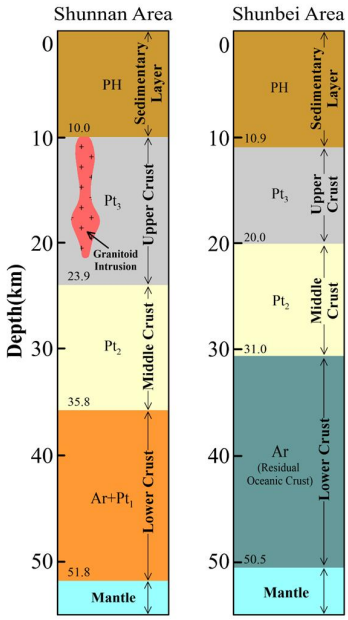

Figure 8: The crustal stratification structure of Shunnan and Shunbei areas.

Table 2: Lithology and heat generation rate of each crustal layer of the basement.

Crustal layer	Upper crust	Middle crust	Lower crust	
Stratigraphic chronology	Neoproterozoic	Mesoproterozoic	Archaean-Paleoproterozoic	Archaean (Residual oceanic crust)
Lithology	Greenschist	Amphibolite, Gneiss	Granulite	Eclogite
Heat generation rate ($\mu W\ m^{-3}$)	0.7	0.4	0.4	0.2

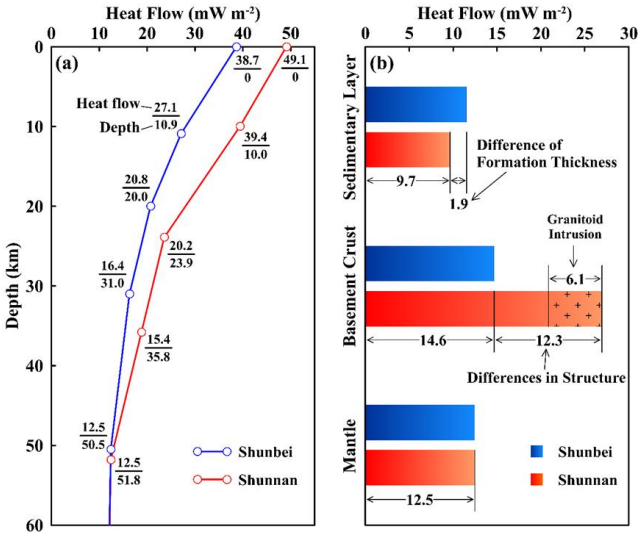

Figure 9: (a) The heat flow of the crust in the Shunnan and Shunbei areas and (b) the histogram of heat flow comparison.

Since it is impossible to directly calculate the heat flow generated by the irregular intrusion, we first calculated the heat flow of the crust in the Shunbei area (Fig. 9a). The heat flow generated by the basement crust in the Shunbei area is 14.7 mW m^{-2}, and the mantle heat flow is 12.5 mW m^{-2}. This mantle heat flow is within the calculation range (6–15 mW m^{-2}) of the Tarim Basin by Liu et al. (2017), and slightly higher than the lower limit (10 mW m^{-2}) of other global cratons (Jaupart and Mareschal 2015a; Xu and Qiu 2017). Under the condition of the same mantle heat flow, it can be calculated that the heat flow generated by the basement crust in the Shunnan area is 26.9 mW m^{-2}. Without considering granitoid intrusions, 20.8 mW m^{-2} can be calculated according to the layered model. The granitoid intrusions in the basement of Shunnan area produced 6.1 mW m^{-2} of heat flow. When the heat generation rate of the upper crustal granitoid is 2.0–4.4 μW m^{-3} (Maystrenko et al. 2015), the equivalent thickness of the intrusion is 1.4–3.1 km. It can be seen from the heat flow comparison histogram that the difference in the structure of the basement crust makes the surface heat flow in the Shunnan area higher than that in the Shunbei area (Fig. 9b), which is the main control factor for the difference in the formation temperature in the study area.

5. DISCUSSION

5.1 Influence of other factors

Tectonic activities, volcanic activities, fluid activities and rapid deposition or denudation in sedimentary basins will produce thermal disturbances to the formation temperature. After the formation of the Tarim Basin, it has experienced multiple tectonic and volcanic activities (Tang 1994; Jia and Wei 2002; Zhang et al. 2007; Cao et al. 2019). The surface heat flow of the basin decreased gradually in Phanerozoic on the whole, and the formation temperature superimposed multiple thermal disturbances under the stable background (Qiu et al. 2012). The duration of the disturbance is related to the time limit, depth, scale and other factors of the thermal event (Wang 2015). The thermal disturbance on the lithosphere scale caused by local heat source lasts no more than 100 Ma (Jaupart and Mareschal 1999). Shuntuoguole area is far away from the edge of the basin. The thermal disturbance generated by the Caledonian Hercynian fault activity and Permian volcanic activity has disappeared. In the Cenozoic era, the region did not experience strong tectonic activity (Qi 2016; Liu et al. 2020).

5.1.1 Rapid sedimentation in Shunbei area

Shunbei area is close to the Neogene sedimentary center of Tarim basin, so the influence of rapid sedimentation should be considered. Rapid sedimentation makes low temperature and shallow rocks buried in deeper and hotter areas in a short geological time. After that, the stratum will gradually warm up, and it will take longer geological time to reach the thermal balance. When it is not reached, the temperature gradient will be lower than that before sedimentation, thus underestimating the surface heat flow (Pauselli et al. 2019). On the contrary, rapid denudation will lead to overestimation of surface heat flow. Husson and Moretti (2002) believed that rapid sedimentation could reduce surface heat flow by 50% (Husson et al. 2002). In the Lion Bay of France, the sedimentation rate of 620m/Ma reduced the surface heat flow by 32% (Lucazeau and Le Douaran 1985). Wangen (1995) showed that when the deposition rate exceeded 250 m/Ma, the surface heat flow would be significantly affected. According to the logging data, since Pliocene (5.3 Ma), ~2.7–3.7 km thick strata have been deposited in the Shunbei area, with a deposition rate of ~540–700 m Ma^{-1}. However, the heat generated by the sediment itself will also increase the temperature of the formation, thus shortening the time required for the formation to reach the thermal balance. When the ratio of heat generation rate to deposition rate is greater than 10-9 WMa m^{-4}, the formation temperature will not be affected by sedimentation (Wangen 1995). According to the calculation, the formation heat generation rate from Pliocene to the surface is 1.25 μW m^{-3}, the ratio range of heat generation rate and deposition rate is ~1.8–2.5×10-9 WMa m^{-4}. Therefore, the rapid sedimentation in the Shunbei area since Pliocene does not reduce the surface heat flow.

5.1.2 Temperature anomaly in shunnan area

The temperature measurement data shows that there is local temperature anomaly in the Shunnan area, and the temperature gradient of wells SN4 and SNP1 is obviously higher than that of other well areas around them (Fig. 3). According to the formation thermal conductivity of representative wells, the surface heat flow near well SN4 block can reach 54 mW m^{-2}.

The temperature gradient of wells SN4 and SNP1 in the Shunnan area is obviously higher than that of other wells around them (Fig. 3). Siliceous rocks possibly of hydrothermal origin were found in the carbonate rocks of Ordovician Yingshan Formation of well SN4 (Chen et al. 2016; Li et al. 2015). The homogenization temperature (up to 250 ℃) of brine inclusions in this stratum is higher than the highest temperature (~190 ℃) experienced by evolution (Chen et al. 2016; Li et al. 2017). Through carbon and oxygen isotope analysis, Lu et al. (2017) confirmed that the fracture of well SN4 experienced hydrothermal activity. Liu et al. (2020) believed that the large-scale hydrothermal migration from late Yanshanian to Himalayan caused the formation near the fault to warm up. After the activity, the current formation has not reached the thermal balance, which shows the high temperature anomaly of the formation near well SN4. However, the temperature curve of well SN4 does not show the characteristics affected by hydrothermal activity. The hydrothermal fluid migrates upward along the deep fault and warms the stratum near the fault. The temperature of shallow stratum will also increase under the conduction. After the activity, the temperature gradient in the deep part should be lower than that in the shallow part during the recovery of thermal stability of the formation (Allen and Allen 2013). The fault of SN4 well breaks down to the basement, and the depth of upward breaking is between ~3–4 km. The temperature gradient of well SN4 at 0–3 km is 22.6 ℃ km^{-1}, while the temperature gradient at 4–6.5 km is as high as 27.0 ℃ km^{-1}, which is obviously not the result of hydrothermal activity. Therefore, we believe that the influence of early hydrothermal activity on the formation temperature has disappeared.

The formation thermal conductivity and heat generation rate at the depth of 4–6.5 km in the Shunnan area are both higher than 0–3 km, so the heat flow at the depth of 4 km in well SN4 is greater than the surface heat flow, which may be caused by diffusion (Jaupart and Mareschal 2015b). In the steady state, the surface heat flow is only sensitive to the change of heat production of rocks in the upper crust (Jaupart 1983). The thickness and thermophysical properties of the sedimentary layers in the Shunnan area are basically consistent. The high temperature anomaly of well SN4 may only be related to the basement granitoid intrusion. We speculate that granitoid intrusions do not exist widely in the basement of Shunnan area, but only in the basement of some areas (near wells SN4 and SNP1).

5.1.3 Basement morphology

The basement morphology refers to the depth distribution characteristics of the basin basement surface. Due to the change of depth and the difference of thermal conductivity, the thermal refraction effect and heat flow redistribution will occur in the process of heat transfer upward (Xiong and Gao 1982; Xiong and Zhang 1984; Balling and Decker 1995; Hyndman and Sass 1966; Hansen and Nielsen 2002). According to the latest research results, the surface heat flow of Tarim Basin is between 27.4 and 66.5 mW m^{-2}, with an average value of ~42.5mW m^{-2} (Qiu et al. 2022). Although scholars generally believe that the distribution of heat flow in the basin is closely related to the basement morphology (Feng et al. 2009; Liu et al. 2017; Chang et al. 2017; Qiu et al. 2022), it does not match, such as the high heat flow in the northern Kuqa Depression (>50 mW m^{-2}), the significant heat flow difference in Bachu Uplift (44 – 56 mW m^{-2}), and the abnormally high heat flow in the southeast uplift (>60 mW m^{-2}). Wang et al. (2003) speculated that the characteristics of the surface heat flow decreasing from Kuqa area to the south may be related to the gradual weakening of the Tianshan Tarim block coupling strength from the piedmont to the interior of the basin. Volcanic rock with andesite and dacite lithology were drilled in the basement of Bachu uplift. Research shows that there once existed a Neoproterozoic magmatic arc (747±12 Ma–755±3 Ma) in Bachu uplift (Li et al. 2018), and it forms a typical calc-alkaline arc magmatic rock association with the basement igneous rock in Tazhong uplift (Li et al. 2003; Yang et al. 2018; Wu et al. 2012). In addition, Permian igneous intrusion also exists in the basement of Bachu uplift (Li et al. 2014). Therefore, the difference of heat flow in Bachu area may be related to the distribution of basement igneous rocks. Chang et al. (2017) believed that the abnormally high heat flow was caused by deep heat upwelling after analyzing the thermal lithosphere thickness and the thermal rheological structure in the southeast uplift area. Therefore, under the thermal background of the cold basin, the formation temperature in the Tarim basin is mainly related to the crustal structure, igneous rock distribution, basin-mountain coupling and deep geodynamic processes, while the basement morphology and thermophysical properties are secondary control factors.

5.2 The cause of low mantle heat flow

Compared with other regions of the continent, the craton has significantly lower heat flow characteristics. The average surface heat flow of Archean craton is ~41 mW m^{-2}, and that of Proterozoic craton is ~55 mW m^{-2} (Andrew et al. 1993; Rudnick et al. 1998). The destroyed craton has a higher mantle heat flow value (>25 mW m^{-2}), while the stable craton has a lower value (<25 mW m^{-2}) (Qiu et al. 2022). In a stable state, the mantle heat flow is related to the thermal conductivity and heat generation rate of the crust and mantle, the thickness of the crust and thermal lithosphere (Jaupart and Mareschal 2015b). The thickness of the thermal lithosphere can be calculated by mantle xenoliths and heat conduction methods. The thickness of the thermal lithosphere of the global stable craton is mainly 150–300 km (Fig. 10a; Xu and Qiu 2017). With reference to the method of Jaupart and Mareschal (2015b), we calculated the linear relationship between the mantle heat flow (Q_m) and the thickness of the thermal lithosphere (h_l) under different crustal heat generation rates (A_c) when the temperature of the bottom boundary of the hot lithosphere (T_l), the thickness of the crust (h_c), and the thermal conductivity of the crust (λ_c) and mantle (λ_m) are constant (Fig. 10b). When other factors remain unchanged, Q_m decreases with the increase of h_l and h_l decreases with the increase of A_c. Under tectonic action, the thickening of lithosphere gradually reduces the overall temperature, and the warming of crust also reduces the thickness of lithosphere. The thickness and temperature of the lithosphere restrict and adjust each other, making it tend to thermal stability.

The crustal heat flow in the Shunnan and Shunbei areas is 36.6 mW m^{-2} and 26.2 mW m^{-2} respectively, and the heat flow ratio of crust to mantle is 2.9 and 2.1 respectively. The thermal structure of the lithosphere in the Shuntogol area is similar to that of the Pibara Craton in Australia (Bodorkos et al. 2004) and the Superior Craton in North America (Lévy and Jaupart 2011), both of which have relatively thick thermal lithosphere (~150–250 km). The average heat generation rates of the crust in the Shunnan and Shunbei areas are 0.71μW m^{-3} and 0.52μW m^{-3} respectively, so the thickness of the thermal lithosphere is ~172 km and ~207 km respectively (Fig. 10b). The variation range of the lithospheric thickness of the Tarim Basin obtained by different methods is ~100–250 km, among which the average lithospheric thickness calculated by geothermic method is ~190km (Cao et al. 2019). The mantle temperature and thermal lithospheric thickness calculated by seismic wave velocity in the Shunnan and Shunbei areas show obvious differences (An and Shi 2006; Sun et al. 2013). Therefore, the low mantle heat flow in the study area is caused by the thicker thermal lithosphere.

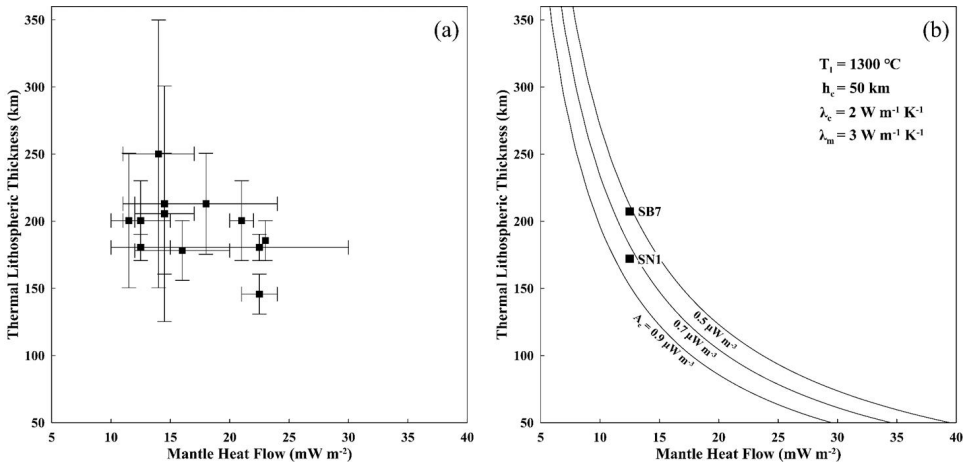

Figure 10: (a) The relationship between the mantle heat flow and the thickness of the thermal lithosphere in the global stable craton (data comes from Xu 2017) and (b) the linear relationship between the mantle heat flow and the thickness of the thermal lithosphere under different crustal heat generation rates.

6. CONCLUSION

The average temperature gradient of 0~5km in the Shunnan and Shunbei areas is 22.5 ℃ km^{-1} and 18.6 ℃ km^{-1} respectively. The thermal conductivity of sedimentary layer of SN1 well in the Shunnan area is 2.44 W m^{-1} K^{-1}, and the heat generation rate is 0.97 μ W m^{-3}. The thermal conductivity of SB7 well sediment in the Shunbei area is 2.30 W m^{-1} K^{-1}, and the heat generation rate is 1.06 μ W m^{-3}.

Shunnan and Shunbei areas have different crustal structure, which are the main controlling factors for the difference of formation temperature. The heat flow generated by the basement crust in the Shunbei area is 14.7 mW m^{-2}, and that in the Shunnan area is 26.9 mW m^{-2}, among which 6.1 mW m^{-2} is generated by granitoid intrusion.

The formation temperature in Shuntuoguole area is in steady state. The thermal disturbance caused by rapid sedimentation in the Shunbei area and hydrothermal activity in the Shunnan area has disappeared. The influence of basement morphology on heat flow in Shuntuoguole area can be ignored. Shuntuoguole area has low mantle heat flow (12.5 mW m^{-2}), which is caused by the thicker thermal lithosphere. The thickness of thermal lithosphere in the Shunnan and Shunbei areas is ~172 km and ~207 km respectively.

REFERENCES

Allen, P.A., Allen, J.R.: Basin analysis: Principles and application to petroleum play assessment(third). *Blackwell Scientific Publications*, (2013), p348.

An, H.T., Li, H.Y., Wang, J.Z.: Tectonic Evolution Its Controlling on Oil Gas Accumulation in the Northern Tarim Basin. *Geotectonica et Metallogenia*, 33, (2009), 142-147 (in Chinese with English abstract).

An, M.J., Shi, Y.L.: Lithospheric thickness of the Chinese continent. *Physics of the Earth and Planetary Interiors*, 159, (2006), 257-266.

Andrew, A., Nyblade, H.N., Pollack.: A global analysis of heat flow from Precambrian terrains: Implications for the thermal structure of Archean and Proterozoic lithosphere. *Journal of Geophysical Research*, 981, (1993), 12207-12218.

Balling, N., Decker, E.R.: Heat flow and thermal structure of the lithosphere across the Baltic Shield and northern Tornquist Zone. *Tectonophysics*, 244, (1995), 13-50.

Beardsmore, G., Cull, J.: Crustal heat flow: a guide to measurement and modelling. *Cambridge University Press*, (2001), p324.

Bodorkos, S., Sandiford, M., Minty, B.R.S., Blewett, R.S.: A high-resolution, calibrated airborne radiometric dataset applied to the estimation of crustal heat production in the Archaean northern Pilbara Craton, Western Australia. *Precambrian research*, 128, (2004), 57-82.

Bucker, C., Rybach, L.: A simple method to determine heat production from gamma-ray logs. *Marine and Petroleum Geology*, 13, (1996), 373-375.

Cao, H.Z., He, L.J., Zhang, L.Y.: Inversion of background thermal history since the formation of the Tarim Craton. *Chinese Journal of Geophysics*, 62, (2019), 236-247 (in Chinese with English abstract).

Chang, J., Qiu, N.S., Xu, W.: Thermal regime of the Tarim Basin, Northwest China: a review. *International geology review*, 59, (2017), 45-61.

Chen, H.H., Lu, Z.Y., Cao, Z.C., Han, J., Yun, L.: Hydrothermal alteration of Ordovician reservoir in northeastern slope of Tazhong uplift, Tarim Basin, Tarim basin. *Acta Petrolei Sinica*, 37, (2016), 43-63 (in Chinese with English abstract).

Chen, Q.L., Xi, B.B., Han, J., Xu, J., Wu, X., Zhu, X.X., Ma, Z.L.: Preservation influence factors of ultra-deep oil reservoirs in Shuntuoguole area, Tarim Basin: evidence from fluid inclusions. *China Petroleum Exploration*, 25, (2020), 121-133 (in Chinese with English abstract).

Cloetingh, S., Van Wees, J.D., Ziegler, P.A., Lenke, L., Beekman, F., Tesauro, M., Förster, A., Norden, B., Kaban, M., Hardebol, N., Bonté, D., Genter, A., Guillou-Frottier, L., Ter Voorde, M., Sokoutis, D., Willingshofer, E., Cornu, T., Worum, G.: Lithosphere tectonics and thermo-mechanical properties: An integrated modelling approach for Enhanced Geothermal Systems exploration in Europe. *Earth-science reviews*, 102, (2010), 159-206.

Deng, S., Li, H.L., Han, J., Cui, D.Y., Zou, R.: Characteristics of differential activities in major strike-slip fault zones their control on hydrocarbon enrichment in Shunbei area its surroundings, Tarim Basin. *Oil Gas Geology*, 39, (2018), 878-888 (in Chinese with English abstract).

Deng, S., Li, H.L., Zhang, Z.P., Wu, X., Zhang, J.B.: Characteristics of the central segment of Shunbei 5 strike-slip fault zone in Tarim Basin its geological significance. *Oil Gas Geology*, 40, (2019), 990-998+1073 (in Chinese with English abstract).

Fan, Q., Fan, T.L., Li, Q.P., Du, Y., Yuan, Y.X.: Sedimentary characteristics and development model of Cambrian gypsum-salt rocks, Tarim Basin. *Geological Review*, 42, (2021), 635-655 (in Chinese with English abstract).

Feng, C.G., Liu, S.W., Wang, L.S., Li, C.: Present-day geothermal regime in Tarim basin, northwest China. Chinese *Journal of Geophysics*, 52, (2009), 2752-2762 (in Chinese with English abstract).

Gao, G.M., Kang, G.F., Li, G.Q., Bai, C.H., Enkin, R.: Crustal magnetic anomaly and Curie surface beneath Tarim Basin, China, and its adjacent area. *Canadian journal of earth sciences*, 52, (2015), 357-367.

Guo, Z.J., Yin, A., Robinson, A., Jia, C.Z.: Geochronology and geochemistry of deep-drill-core samples from the basement of the central Tarim basin. *Journal of Asian Earth Sciences*, 25, (2005), 45-56.

Hansen, D.L., Nielsen, S.B.: Does thermal weakening explain basin inversion? Stochastic modelling of the thermal structure beneath sedimentary basins. *Earth and planetary science letters*, 198, (2002), 113-127.

Hasterok, D., Chapman, D.S.: Heat production and geotherms for the continental lithosphere. *Earth and Planetary Science Letters*, 307, (2011), 59-70.

He, B.Z., Jiao, C.L., Cai, Z.H., Zhang, M., Gao, A.R.: A new interpretation of the high aeromagnetic anomaly zone in central Tarim Basin. *Geology of China*, 38, (2011), 961-969 (in Chinese with English abstract).

He, B.Z., Jiao, C.L., Huang, T.Z., Zhou, X.G., Cai, Z.H., Cao, Z.C., Jiang, Z.Z., Cui, J.W., Yu, Z.Y., Chen, W.W., Liu, R.H., Yun, X.R., Hao, G.M.: Structural architecture of Neoproterozoic rifting depression groups in the Tarim Basin their formation dynamics. *Science China(Earth Sciences)*, 49, (2019), 635-655 (in Chinese with English abstract).

He, D.F., Zhou, X.Y., Yang, H.J., Guan, S.W., Zhang, C.J.: Formation mechanism tectonic types of intracratonic paleo-uplifts in the Tarim basin. *Earth Science Frontiers*, (2008), pp. 207-221 (in Chinese with English abstract).

Hsü, K.J.: Isostasy and a theory for the origin of geosynclines. *American Journal of Science*, 256, (1958), 305-327.

Huang, T.Z.: Structural interpretation petroleum exploration targets in northern slope of middle Tarim Basin. *Petroleum Geology Experiment*, 36, (2014), 257-267 (in Chinese with English abstract).

Husson, L., Moretti, I.: Thermal regime of fold and thrust belts—an application to the Bolivian subAndean zone. *Tectonophysics*, 345, (2002), 253-280.

Hyndman, R. D., Sass, J. H.: Geothermal measurements at Mount Isa, Queensland. *Journal of Geophysical Research*, 71, (1966), 587-601.

Jaupart, C.: Horizontal heat transfer due to radioactivity contrasts: causes and consequences of the linear heat flow relation. *Geophysical Journal of the Royal Astronomical Society*, 75, (1983), 411---435435.

Jaupart, C., Mareschal, J.C.: The thermal structure and thickness of continental roots. *Lithos*, 48, (1999), 93-114.

Jaupart, C., Mareschal, J.C.: Treatise on Geophysics(Second Edition): Heat Flow and Thermal Structure of the Lithosphere, *Elsevier, Oxford*, (2015a), pp. 217-253.

Jaupart, C., Mareschal, J.C.: Treatise on Geophysics(Second Edition): Constraints on Crustal Heat Production from Heat Flow Data. *Elsevier, Oxford*, (2015b), pp. 53-73.

Jaupart, C., Mareschal, J.C.: Heat Generation and Transport in the Earth. *Cambridge University Press*, (2010), p476.

Jia, C.Z., Wei, G.: Tectonic characteristics hydrocarbon potential of Tarim Basin. *Chinese Science Bulletin*, S1, (2002), 1-8 (in Chinese with English abstract).

Jiao, F.Z.: Significance of oil gas exploration in NE strike-slip fault belts in Shuntuoguole area of Tarim Basin, Tarim Basin. *Oil Gas Geology*, 38, (2017), 831-839 (in Chinese with English abstract).

Kuang, X.T., Zhu, X.Y., Ning, F.X., Li, W, Zheng, Q.F., Li, B., Zhou, D.Q.: Aeromagnetic-Imaged Basement Fault Structure of the Eastern Tarim Basin and Its Tectonic Implication. *Frontiers in Earth Scienc*, 9, (2022), 825498.

Lévy, F., Jaupart, C.: Temperature and rheological properties of the mantle beneath the North American Craton from an analysis of heat flux and seismic data. *Journal of Geophysical Research*, 116, (2011), B01408.

Li, B.L., Guan, S.W., Li, C.X., Wu, G.H., Yang, H.J., Han, J.F., Luo, C.S., Miao, J.J.: Paleo-tectonic Evolution Deformation Features of the Lower Uplift in the Central Tarim Basin. *Geological Review*, 55, (2009), 521-530 (in Chinese with English abstract).

Li, P.J., Chen, H.H., Tang, D.Q., Cao, Z.C., Lu, Z.Y., Su, A., Wei, H.D.: Coupling Relationship between NE Strike-slip Faults Hypogenic Karstification in Middle-lower Ordovician of Shunnan Area, Tarim Basin, Northwest China. *Journal of Earth Science*, 42, (2017), 93-104 (in Chinese with English abstract).

Li, W.S., Li, J.H., Zhou, X.B., Li, W.B., Wang, H.H., Yang, J.Y.: Genesis of High Aeromagnetic Anomaly Zone in Central Tarim Basin: New Evidence from Seismic Profiles. *Acta Scientiarum Naturalium Universitatis Pekinensis*, 50, (2014), 281-287 (in Chinese with English abstract).

Li, X.J., Wang, Y., Li, H.L., Gao, S.L., Yang, L.W., Yue, Y., Yan, Q.R., Jiang, W.: Bachu uplift in the central Tarim Basin based on Neoproterozoic continental arc: New lines of evidence from drilled andesite dacite. *Acta Petrologica Sinica*, 34, (2018), 2140-2164 (in Chinese with English abstract).

Li, X.L., Liu, S.W., Feng, C.G.: Thermal properties of sedimentary rocks in the Tarim Basin, northwestern China. *AAPG bulletin*, 103, (2019), 1605-1624.

Li, Y.J., Song, W.J., Wu, G.Y., Wang, Y.F., Li, Y.P., Zheng, D.M.: Jinning granodiorite and diorite deeply concealed in the central Tarim Basin. *Science in China. Series D, Earth sciences*, 48, (2005), 2061-2068.

Li, Y.Q., Li, Z.L., Xing, Y., Langmuir, C.H., Santosh, M., Yang, S.F., Chen, H.L., Tang, Z.L., Song, B., Zuo, S.Y., Xu, Y.G., Wang, C.Y., Shen, S.Z.: Origin of the Early Permian zircons in Keping basalts and magma evolution of the Tarim large igneous province, northwestern China. *Lithos*, 204, (2014), 47-58.

Liu, S.W., Li, X.L., Hao, C.Y., Li, X.D.: Heat flow, deep formation temperature thermal structure of the Tarim Basin, Northwest China. *Earth Science Frontiers*, 24, (2017), 41-55 (in Chinese with English abstract).

Liu, Y.C., Qiu, N.S., Li, H.L., Ma, A.L., Chang, J., Jia, J.K.: Terrestrial heat flow and crustal thermal structure in the northern slope of Tazhong uplift in Tarim Basin. *Geothermics*, 83, (2020), 101709.

Lu, Z.Y., Chen, H.H., Qing, H.R., Chi, G., Chen, Q.L., You, D.H., Yin, H., Zhang, S.Y.: Petrography, fluid inclusion and isotope studies in Ordovician carbonate reservoirs in the Shunnan area, Tarim basin, NW China: Implications for the nature and timing of silicification. *Sedimentary geology*, 359, (2017), 29-43.

Lucazeau, F., Le Douaran, S.: The blanketing effect of sediments in basins formed by extension: a numerical model. Application to the Gulf of Lion and Viking graben. *Earth and planetary science letters*, 74, (1985), 92-102.

Ma, Q.Y., Sha, X.G., Li, Y.L., Zhu, X.X., Yang, S.J., Li, H.L.: Characteristics of strike-slip fault its controlling on oil in Shuntuoguole region, middle Tarim Basin. *Petroleum Geology Experiment*, 34, (2012), 120-124 (in Chinese with English abstract).

Ma, Y.S., Cai, X.Y., Yun, L., Li, Z.J., Li, H.L., Deng, S., Zhao, P.R.: Practice, Practice theoretical technical progress in exploration development of Shunbei ultra-deep carbonate oil gas field, Tarim Basin, NW China. *Petroleum Exploration Development*, 49, (2022), 1-17 (in Chinese with English abstract).

Mareschal, J.C., Jaupart, C.: Radiogenic heat production, thermal regime and evolution of continental crust. *Tectonophysics*, 609, (2013), 524-534.

Maystrenko, Y.P., Olesen, O., Elvebakk, H.K.: Indication of deep groundwater flow through the crystalline rocks of Southern Norway. *Geology(Boulder)*, 43, (2015), 327-330.

Melouah, O., Eldosouky, A.M., Ebong, E.D.: Crustal architecture, heat transfer modes and geothermal energy potentials of the Algerian Triassic provinces. *Geothermics*, 96, (2021), 102211.

Pauselli, C., Gola, G., Mancinelli, P., Trumpy, E., Saccone, M., Manzella, A., Ranalli, G.: A new surface heat flow map of the Northern Apennines between latitudes 42.5 and 44.5 N. *Geothermics*, 81, (2019), 39-52.

Qi, L.X.: Oil gas breakthrough in ultra-deep Ordovician carbonate formations in Shuntuoguole uplift, Tarim Basin. *China Petroleum Exploration*, 21, (2016), 38-51 (in Chinese with English abstract).

Qiu, N.S., Chang, J., Zhu, C.Q., Liu, W., Zuo, Y.H., Xu, W., Li, D.: Thermal regime of sedimentary basins in the Tarim, Upper Yangtze and North China Cratons, China. *Earth-Science Reviews*, 224, (2022), 103884.

Qiu, N.S., Chang, J., Zuo, Y.H., Wang, J.Y., Li, H.L.: Thermal evolution and maturation of lower Paleozoic source rocks in the Tarim Basin, northwest China. *AAPG Bulletin*, 96, (2012), 789-821.

Roy, R., Blackwell, D., Birch, F.: Heat generation of plutonic rocks and continental heat flow provinces. *Earth and Planetary Science Letters*, 5, (1968), 1-12.

Rudnick, R.L., Mcdonough, W.F., O'Connell, R.J.: Thermal structure, thickness and composition of continental lithosphere. *Chemical Geology*, 145, (1998), 395-411.

Shi, K.B., Liu, B., Jiang, W.M., Luo, Q.Q., Gao, X.Q.: Nanhua-Sinian tectono-sedimentary framework of Tarim Basin, NW China. *Oil Gas Geology*, 39, (2018), 862-877 (in Chinese with English abstract).

Sippel, J., Scheck-Wenderoth, M., Lewerenz, B., Klitzke, P.: Deep vs. shallow controlling factors of the crustal thermal field–insights from 3D modelling of the Beaufort-Mackenzie Basin(Arctic Canada). *Basin research*, 27, (2015), 102-123.

Sun, Y.J., Dong, S.W., Zhang, H., Li, H., Shi, Y.L., Ivanov, A.V., Deverchere, J., Ernst, R., Gladkochub, D.P.: 3D thermal structure of the continental lithosphere beneath China and adjacent regions. *Journal of Asian earth sciences*, 62, (2013), 697-704.

Tang, L.J.: Tectonic evolution structural style of Tarim basin. *Journal of Earth Science*, (1994), pp. 742-754 (in Chinese with English abstract).

Teng, J.E., Zhang, Z.J., Zhang, X.K., Wang, C.Y., Gao, R., Yang, B.J., Qiao, Y.H., Deng, Y.F.: Investigation of the Moho discontinuity beneath the Chinese mainland using deep seismic sounding profiles. *Tectonophysics*, 609, (2013), 202-216.

Wan, Y.L., Gu, Y., Fu, Q., Zhuang, X.B., Shao, Z.B., Ding, Y.: Characteristics of geothermal-geopressure field its implications for the process of hydrocarbon distribution in deep Ordovician stratum in the Shunnan-Gulong area of Tarim Basin. *Journal of Mineralogy Petrology*, 37, (2017), 74-83 (in Chinese with English abstract).

Wang, J.Y.: Geothermy its application. Beijing, *Science Press*, (2015), p115 (in Chinese with English abstract).

Wang, J., Wang, J.A., Shen, J.Y., Qiu, N.S.: Terrestrial heat flow in Tarim basin. *Journal of Earth Science*, 4, (1995), 399-404 (in Chinese with English abstract).

Wang, L.S., Li, C., Liu, S.W., Li, H., Xu, M.J.: Geothermal gradient distribution characteristics of Kuqa foreland basin in the northern margin of Tarim basin. *Chinese Journal of Geophysics*, (2003), pp. 403-407 (in Chinese with English abstract).

Wang, T.F., Jin, Z.K., Yu, X.X., Cheng, R.H., Song, X., Yang, B.J., Li, S., Shi, S.T.: New Discovery of Upper Crustal High- and Low-Velocity Belts and High-Velocity Core in the Tarim Basin. *Acta geologica Sinica(Beijing)*, 93, (2019), 229-230.

Wangen, M.: The blanketing effect in sedimentary basins. *Basin research*, 7, (1995), 283-298.

Wu, G.H., Li, H.W., Xu, Y.L., Su, W., Chen, Z.Y., Zhang, B.S.: The tectonothermal events, architecture evolution of Tarim craton basement palaeo-uplifts. *Acta Petrologica Sinica*, 28, (2012), 2435-2452 (in Chinese with English abstract).

Xiong, L.P., Gao, W.A.: Characteristics of geothermal field in uplift depression areas. *Chinese Journal of Geophysics*, (1982), pp. 448-456 (in Chinese with English abstract).

Xiong, L.P., Zhang, J.M.: Mathematical simulation of refraction redistribution of heat flow. *Chinese Journal of Geology*, (1984), pp. 445-454 (in Chinese with English abstract).

Xu, B.R.: Distribution of bedrock in Tarim basin according to aeromagnetic interpretation. *Journal of Xi'an Shiyou University (Natural Science Edition)*, (1997), pp. 5-8+42+1 (in Chinese with English abstract).

Xu, J.H.: Residual back arc basin its identification criteria examples. *Acta Petrolei Sinica*, (1993), pp. 1-13 (in Chinese with English abstract).

Xu, M.J., Wang, L.S., Zhong, K., Hu, D.Z., Li, H., Hu, X.Z.: Features of Gravitational and Magnetic Fields in the Tarim Basin and Basement Structure Analysis. *Geological Journal of China Universities*, (2005), pp. 585-592 (in Chinese with English abstract).

Xu, W., Qiu, N.S.: Heat flow and destabilized cratons: a comparative study of the North China, Siberian, and Wyoming cratons. *International geology review*, 59, (2017), 884-904.

Xu, X., Xiong, S.Q., Tanaka, A., Zheng, Q., Kuang, X.T., Zhu, X.Y., Zhou, D.Q., Zheng, Q.F., Wan, J.H., Yu, X.Z., Wang, B.D.: Thermal Structure Beneath the Tarim Craton and Its Tectonic Implications. *Frontiers in earth science(Lausanne)*, (2021), p9.

Yang, H.J., Wu, G.H., Kusky, T.M., Chen, Y.Q., Yang, X.: Paleoproterozoic assembly of the North and South Tarim Terranes; new insights from deep seismic profiles and Precambrian granite cores. *Precambrian research*, 305, (2018), 151-165.

Yang, M., Yu, P., Zhu, G.Y., Zhang, L.L., Yan, L., Zhao, C.J., Ma, D.B., Chen, Z.Y.: Gravity-magnetic-magnetotelluric joint inversion method coupled with seismic constraint information and its application: Case studyof the analysis of deep geological structure in Tarim Basin. *Natural Gas Geoscience*, 33, (2022), 168-179 (in Chinese with English abstract).

Yang, S.J., Shi, J., Xu, S.Z., Zhang, L., Hu, Z.Z.: Geological structure characteristics of ultra-deep paleoplates in Tarim Basin. *2021 Geophysical Exploration Technology Seminar of Chinese Petroleum Society, Chengdu, Sichuan, China*, (2021), pp.1424-1427 (in Chinese with English abstract).

Yang, W.C., Xu, Y.X., Zhang, L.L., Yu, C.Q., Yu, P., Zhang, B.Z., Yang, B.: Magnetotellruic Investigation 3D Lithospheric Structures in the Tarim Terrane. *Acta Geologica Sinica*, 89, (2015), 1151-1161 (in Chinese with English abstract).

Yang, X., Xu, X.H., Qian, Y.X., Chen, Q.L., Chu, C.L., Jiang, H.J.: Discussion on regional differences of basement composition of the Tarim Basin, NW China. *Geotectonica et Metallogenia*, (2014), pp. 544-556 (in Chinese with English abstract).

Zhang, G.Y., Zhao, W.Z., Wang, H.J., Li, H.H., Liu, L.: Multicycle tectonic evolution composite petroleum systems in the Tarim Basin. *Oil Gas Geology*, (2007), pp. 653-663 (in Chinese with English abstract).

Zhang, J.B., Zhang, Z.P., Wang, B.F., Deng, S.: Development pattern prediction of induced fractures from strike-slip faults in the Shunnan area, Tarim Basin. *Oil Gas Geology*, 39, (2018), 955-963+1055 (in Chinese with English abstract).

Zheng, B.H., Zhu, W.B., Jahn, B.M., Shu, L.S., Zhang, Z.Y., Su, J.B.: Subducted Precambrian oceanic crust: geochemical and Sr-Nd isotopic evidence from metabasalts of the Aksu blueschist, NW China. *Journal of the Geological Society*, 167, (2010), 1161-1170.

Zhou, W.G., Fan, D.W., Liu, Y.G., Xie, H.S.: Measurements of wave velocity and electrical conductivity of an amphibolite from southwestern margin of the Tarim Basin at pressures to 1.0 GPa and temperatures to 700 °C: comparison with field observations. *Geophysical Journal International*, 187, (2011), 1393-1404.

Zhou, X.J., Tian, W.Z., Wu, G.H., Damian Nance, R., Chen, Y.Q., Zhao, Y.W., Yan, W., Zhang, Y.Q.: Geochemistry and U-Pb-Hf zircon systematics of Cryogenian syn-rift magmatic rocks from the subsurface of the Tarim Craton: Implications for subduction-related continental rifting. *Precambrian Research*, 377, (2022), 106733.

Zhu, G.Y., Chen, Z.Y., Chen, W.Y., Yan, H.H., Zhang, P.H.: Revisiting to the Neoproterozoic tectonic evolution of the Tarim Block, NW China. *Precambrian research*, 352, (2021), 106013.